Diffusion-weighted Magnetic Resonance Imaging Findings in a Patient with Struma Ovarii

TOHRU TAKESHITA, TERUHISA NINOI, TETUNORI MAEBAYASHI, KUNIHIKO DOH, SHIGEO HASHIMOTO, and YUKIO MIKI

TOHRU TAKESHITA, TERUHISA NINOI, TETUNORI MAEBAYASHI et al. Diffusion-weighted Magnetic Resonance Imaging Findings in a Patient with Struma Ovarii. Osaka City Medical Journal. 2014, 60, 45-52

Osaka City Med. J. Vol. 60, 45-52, 2014

Diffusion-weighted Magnetic Resonance Imaging Findings in a Patient with Struma Ovarii

Tohru Takeshita[1)], Teruhisa Ninoi[2)], Tetunori Maebayashi[2)], Kunihiko Doh[3)], Shigeo Hashimoto[4)], and Yukio Miki[1)]

Department of Radiology[1)], Osaka City University Medical School; and Departments of Radiology[2)], Obstetrics and Gynecology[3)], and Pathology[4)], Perfect Liberty Hospital

Abstract

In this report, the magnetic resonance imaging (MRI) appearance of struma ovarii (SO) in a patient who underwent diffusion-weighted imaging (DWI) of the pelvis and subsequent histological analysis is described. The solid portion of SO showed a high apparent diffusion coefficient (ADC) value, indicating unrestricted diffusion, and each loculus of SO showed different ADC values due to the different viscosity of the cyst contents in each loculus. These unique and characteristic DWI findings may serve as a helpful sign in making the correct diagnosis of SO when DWI findings are interpreted in conjunction with conventional MRI findings.

Key Words: Apparent diffusion coefficient; Diffusion-weighted imaging; Magnetic resonance imaging; Ovarian tumor; Struma Ovarii

Introduction

Recent advances in magnetic resonance imaging (MRI) technology have enabled us to obtain high-quality diffusion-weighted (DW) MRI in the body and pelvis[1)]. Thus, DW imaging (DWI) sequences can now be included in routine MRI examinations for various gynecological disorders. Many investigators have recently reported the diagnostic value of DW MRI and the corresponding apparent diffusion coefficient (ADC) values for the characterization of various histological ovarian lesions[2-8)]. To the best of our knowledge, there has been one report concerning DWI and ADC values of struma ovarii (SO) in the English literature[9)]. A case of SO is reported, and the MRI findings are correlated with the pathological findings. Furthermore, the value of DW MRI and ADC values for the diagnosis of SO is discussed.

Case Report

A 51-year-old woman, gravida 3, para 3, complained of abdominal distension. Her past medical history was unremarkable. Laboratory data were unremarkable. Serum hormone and tumor marker levels were within normal limits. Transvaginal sonography revealed a complex solid and cystic mass

Received June 13, 2013; accepted November 26, 2013.
Correspondence to: Tohru Takeshita, MD.
Department of Radiology, Osaka City University, Graduate School of Medicine,
1-4-3 Ashahimachi, Abeno-ku, Osaka 545-8585, Japan
Tel: +81-6-6645-3831; Fax: +81-6-6646-6655
E-mail: ttakeshita@med.osaka-cu.ac.jp

at the left adnexal region. For further evaluation of the left adnexal mass, pelvic MRI was performed. MR images showed a lobulated complex solid and cystic mass at the left adnexa. The mass was

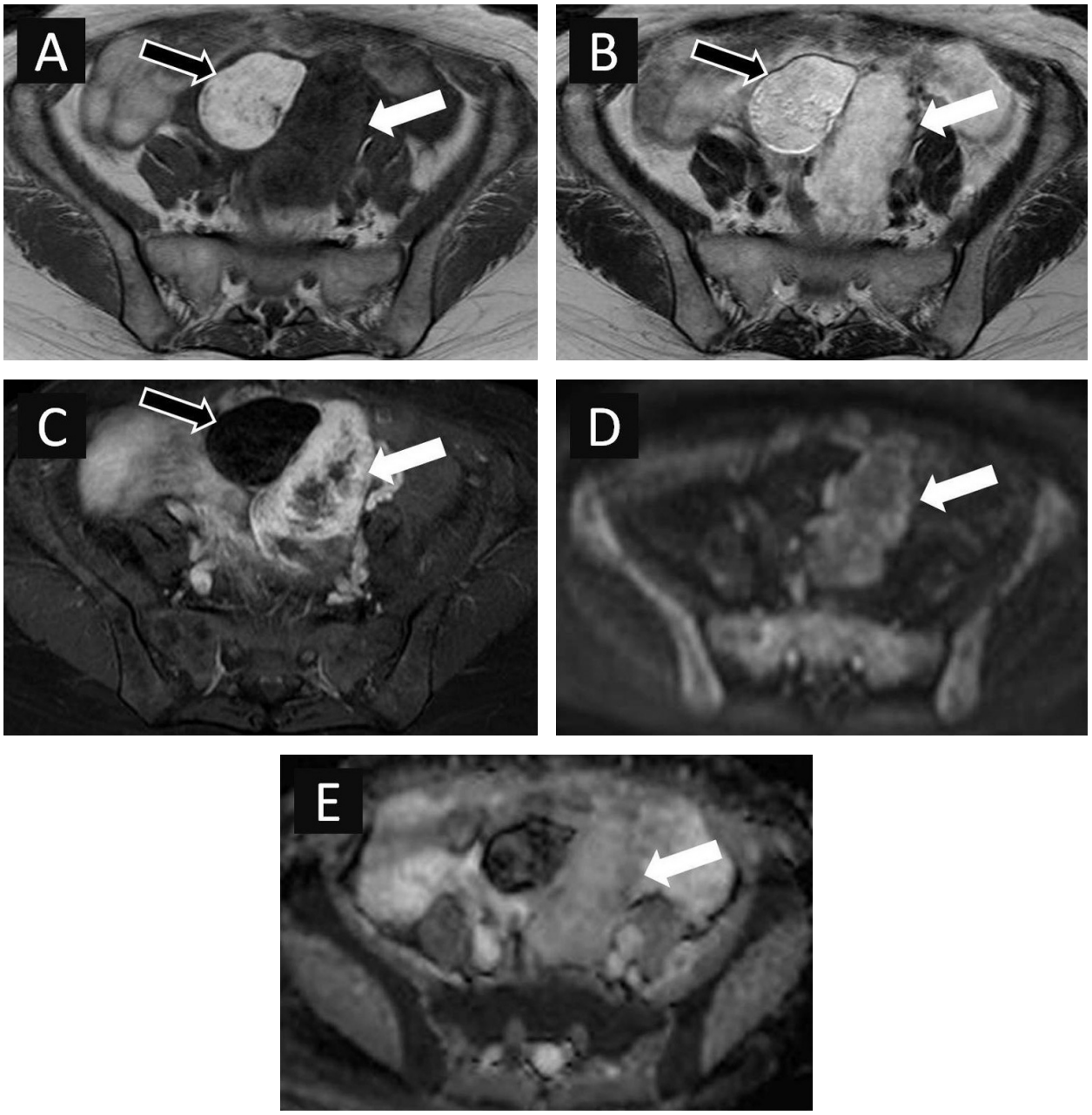

Figure 1. A, On this axial T1-weighted spin-echo MR image, the lateral part of the tumor shows low signal intensity (white arrow). Note that the medial part of the tumor shows high signal intensity (black arrow). B, On this axial T2-weighted fast spin-echo MR image at the same level as in Figure 1A, the lateral part of the tumor shows heterogeneous, high signal intensity (white arrow). Note that the medial part of the tumor shows high signal intensity (black arrow). C, On this axial contrast-enhanced fat-suppressed T1-weighted fast spin-echo MR image at the same level as in Figures 1A and 1B, the lateral part of the tumor shows intense enhancement (white arrow), suggesting a solid appearance with a hypervascular nature. Note that the medial part of the tumor shows signal loss, indicating the presence of macroscopic fat within the lesion (black arrow). D, On this axial diffusion-weighted MR image (b=1000 second/mm^2) at the same level as in Figures 1A, 1B, and 1C, the lateral part of the tumor shows slightly high signal intensity (white arrow). E, The corresponding apparent diffusion coefficient (ADC) map image at the same level as in Figure 1D. On this axial ADC map image, the lateral part of the tumor shows high signal intensity (white arrow). The calculated ADC value of the lateral part of the tumor is 2.45×10^{-3} mm^2/s.

composed of three components. The medial component of the mass showed high signal intensity on both T1- and T2-weighted images and signal loss on gadolinium-enhanced fat-suppressed T1-weighted images, indicating a macroscopic, fat-containing lesion (Figs. 1A, 1B, and 1C). The lateral component of the mass showed low signal intensity on T1-weighted imaging and heterogeneous high signal intensity on T2-weighted imaging (Figs. 1A and 1B). On gadolinium-enhanced fat-suppressed T1-weighted imaging, the lateral component showed intense enhancement (Fig. 1C). The degree of enhancement of the lateral component was greater than that of the uterine myometrium, indicating the solid and hypervascular nature of the tumor. On DWI, the lateral component showed a slightly high signal intensity (Fig. 1D). The degree of signal intensity of the lateral component was isointense to the uterine myometrium. On the ADC map image, the lateral component showed high signal intensity (Fig. 1E). The calculated ADC value was 2.45×10^{-3} mm^2/s. The inferior component of the mass showed a multiloculated cystic appearance. The signal intensity of each loculus varied from low to high signal intensity on both T1- and T2-weighted imaging (Figs. 2A and 2B). Some loculi showing very high signal intensity on T1-weighted imaging and very low signal intensity on T2-

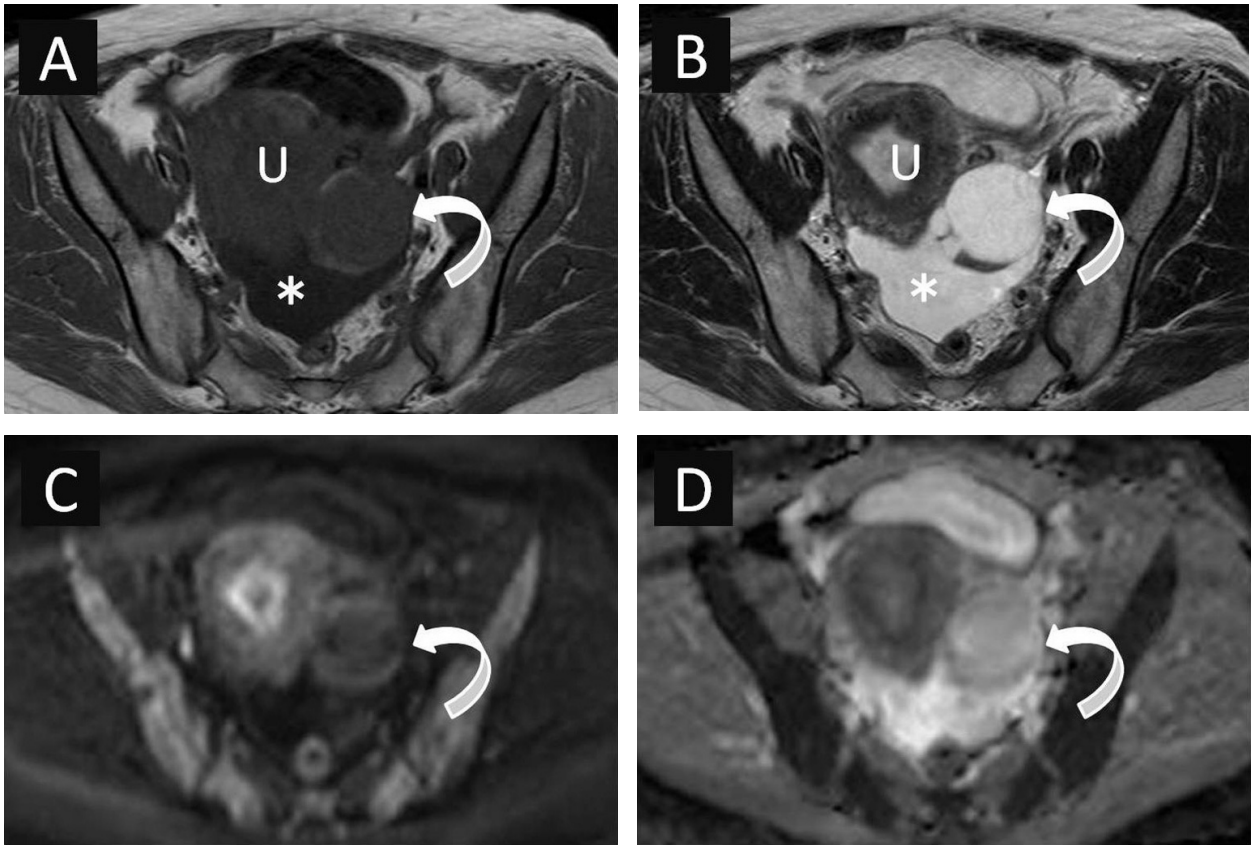

Figure 2. A, On this axial T1-weighted spin-echo MR image at a more caudal level than in Figure 1A, the inferior part of the tumor shows a multicystic appearance (curved white arrow). Note that the signal intensity of each loculus is different, varying from high to low signal intensity. U, uterus; *asterisk*, ascites in the pouch of douglas. B, On this axial T2-weighted fast spin-echo MR image at the same level as in Figure 2A, the inferior part of the tumor shows a multicystic appearance (curved white arrow). Note that the signal intensity of each loculus is different, varying from high to low signal intensity. U, uterus; *asterisk*, ascites in the pouch of douglas. C, On this axial diffusion-weighted MR image (b=1000 second/mm^2) at the same level as in Figures 2A and 2B, each loculus shows varied signal intensity (curved white arrow). D, The corresponding apparent diffusion coefficient (ADC) map image at the same level as in Figure 2C. On this axial ADC map image, the loculi show various signal intensity (curved white arrow). The calculated ADC values of each loculus are different from each other, ranging from 1.65×10^{-3} mm^2/s to 2.66×10^{-3} mm^2/s.

weighted imaging were present. On DWI, the signal intensity of each loculus varied from low to high signal intensity (Fig. 2C). On the ADC map image, the signal intensity of each loculus varied from low to high signal intensity (Fig. 2D). The calculated ADC values were from 1.65×10^{-3} mm^2/s to 2.66×10^{-3} mm^2/s. Additionally, minimal ascites was seen in the pouch of Douglas on MRI. There was no lymphadenopathy or evidence of dissemination. Both the uterus and right ovary showed a normal appearance. SO associated with a dermoid cyst of the left ovary was suggested as a possible diagnosis. The patient had no symptom of hyperthyroidism, and her serum free-T3 and free-T4 levels were within normal limits. A chest radiograph showed no pleural effusion. At surgery, a lobulated mass of the left ovary was identified, and a left salpingo-oophorectomy was performed. Grossly, the resected left ovarian mass had a complex solid and cystic appearance. The cut surface of the medial compartment of the mass was cystic, and the cyst lumen was filled with keratinous debris, sebaceous material, and hair. Histologically, the cyst wall was lined by stratified squamous epithelium with sebaceous glands (skin appendages). Cartilage and mature adipose tissues were also observed. These findings were consistent with a mature cystic teratoma (dermoid cyst) (Fig. 3A). On the other hand, the cut surface of the lateral compartment of the mass was predominantly solid and glistening brown in color. Histologically, this component was composed of thyroid tissue containing numerous follicles of variable size with colloid (Fig. 3B). The cut surface of the inferior compartment of the mass was totally cystic with multiple loculi. Histologically, this component was also composed of thyroid tissue containing some follicles with colloid. From these histopathologic findings, a final diagnosis of SO associated with a dermoid cyst was made. The patient's postoperative course was uneventful, and the patient is well two years after the operation.

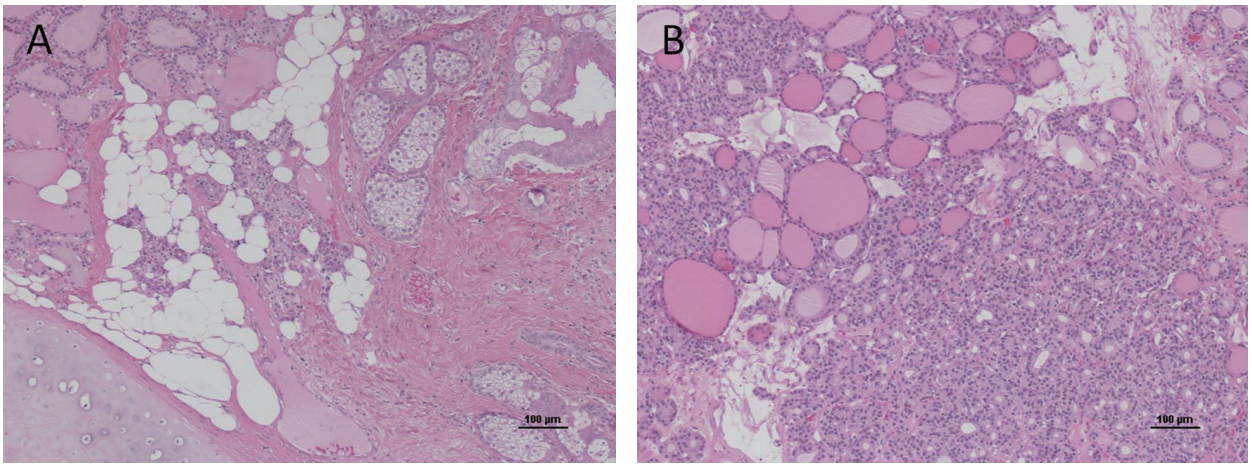

Figure 3. A, Histological specimen of the medial part of the tumor showing a dermoid cyst (mature cystic teratoma) composed of sebaceous glands, skin appendages, cartilages, and mature adipose tissues. (Hematoxylin and eosin stain, original magnification, ×10) Scale bar=100 μm. B, Histological specimen of the lateral part of the tumor showing struma ovarii consisting of thyroid tissue composed of numerous thyroid follicles of various sizes. Note that colloid-containing follicles with varying sizes are observed. (Hematoxylin and eosin stain, original magnification, ×10) Scale bar=100 μm.

Discussion

SO is the most common type of monodermal teratoma, accounting for nearly 3% of all ovarian teratomas[10-12]. SO is defined as an ovarian tumor that is composed entirely or predominantly of thyroid tissue[10-12]. Moreover, SO is sub-classified into two forms, pure and impure. The pure form is

composed entirely of thyroid tissue, while the impure form is associated with a dermoid cyst in the same ovary but with the struma component comprising more than 50% of the tumor volume, or it forms a grossly recognizable thyroid tissue component of a dermoid cyst[12]. Using this classification, the present SO was an impure form.

SO is usually unilateral but is often associated with dermoid cyst in the contralateral ovary. The majority of patients with SO are asymptomatic, but when symptoms are present, patients with SO usually have non-specific symptoms such as abdominal or pelvic pain, abdominal distention, and so on[12]. In a small number of cases, SO may be associated with unusual clinical manifestations including pseudo-Meigs syndrome (SO associated with pleural effusion and ascites) and hyperthyroidism[12,13]. Most cases of SO are benign and can treated by cystectomy or by unilateral salpingo-oophorectomy. Rarely, thyroid-type carcinomas originating in SO have been reported[10,11].

MRI and computed tomography (CT) are useful imaging modalities for the detection and characterization of various benign and malignant ovarian lesions. Typical MRI findings of SO are multilocular cystic masses with a multilobulated surface. In most cases of SO, some solid components are present as a thickened septum or thickened cyst walls. However, the size of the solid component is variable in individual cases. The cyst contents in each loculus show a variety of signal intensities on both T1- and T2-weighted MRI. SO frequently includes loculi of low intensity on T2-weighted images and high intensity on T1-weighted images. On CT, typical imaging findings of SO are a multilocular cystic mass characterized by the presence of a high attenuation area and curvilinear calcification. On both contrast-enhanced MRI and contrast-enhanced CT images, the solid components of SO show intense enhancement, corresponding to the hypervascular nature of the tumor[14,15]. The MRI findings of the present case were compatible with previously reported MRI findings of SO, except for the presence of an abundant solid component as part of the tumor. Kuzuhara et al reported one case of SO that presented as a predominantly solid mass on MRI in the Japanese literature[16]. In contrast, some cases of SO presenting as a unilocular cystic mass have also been reported[17]. Radiologists should be aware that SO has a broad spectrum of morphological appearances, from a purely cystic appearance to a complex solid and cystic appearance and to a predominantly solid appearance.

Recently, the use of DWI and corresponding ADC maps has been evaluated for assessment of various benign and malignant ovarian lesions[2-8]. To the best of our knowledge, there has been one report concerning DWI and the ADC values of SO in the English literature[9]. Zang et al recently reported the mean ADC value for four cases of SO as 2.58×10^{-3} mm^2/s[9]. Unfortunately, this study did not provide details concerning the location of region of interest placement for the ADC measurement of SO, and analysis of the correlation between DWI and pathological findings was not available. The mean ADC value for the solid portion of the SO in the present case was 2.45×10^{-3} mm^2/s. On the other hand, the mean ADC values for the cystic portion of the SO in the present case ranged from 1.65×10^{-3} mm^2/s to 2.66×10^{-3} mm^2/s.

In the present case, there were two unique DWI findings. The first unique finding was the high ADC value for the solid portion of the SO. Theoretically, in most malignant tumors including ovarian cancers, diffusion is restricted due to increased cellular density and decreased extracellular matrix volume, which impede free motion of water molecules. For this reason, malignant tumors including ovarian cancers show significantly restricted diffusion on DWI and low signal intensity on corresponding ADC map images (i.e. a low ADC value)[1]. Why did the solid portion of the SO show

a high ADC value? We assume that this might have been related to the pathological findings of the solid portion of SO. Pathologically, the solid portion of the SO consisted of normal-appearing thyroidal tissue composed of various sized thyroid follicles. These follicles were filled with eosinophilic colloid material. Numerous follicles filled with colloid in SO increase the intra-tumoral water content, which may cause T2-prolongation and increase the ADC value.

Several investigators reported the ADC values for the solid components of various histologically benign and malignant ovarian lesions[2,3]. The mean ADC values for solid components of benign ovarian lesions ranged from $1.15\pm0.55\times10^{-3}$ mm²/s to $1.47\pm0.42\times10^{-3}$ mm²/s, and those for malignant ovarian lesions ranged from $1.14\pm0.28\times10^{-3}$ mm²/s to $1.41\pm0.34\times10^{-3}$ mm²/s[2,3]. The mean ADC value for the solid portion of the SO in the present case was higher than the previously reported mean ADC values for solid components of benign and malignant ovarian lesions. This high ADC value of the solid component in SO may be an additional useful finding for differentiating SO from other predominantly solid ovarian lesions or complex solid and cystic ovarian lesions.

The second unique finding in the present case was the different ADC values among each loculus of SO. The reason for the different ADC values among each loculus in SO can be explained by the difference in the viscosity of cyst contents in each loculus in SO. In previous MRI-pathological correlation studies of SO, some loculi showing low intensity on T2-weighted MRI were considered to contain highly gelatinous colloid material containing thyroid hormones with iodine compounds. In contrast, some loculi showing high intensity on T2-weighted MRI are considered to contain diluted colloid material[14,15]. It is well known that many factors affect water diffusion in biologic tissues, and fluid viscosity is one of the important factors[1]. Impeded or restricted diffusion can be seen in highly viscous cystic lesions, such as ovarian endometrial cysts or tubo-ovarian abscesses[2,4,18]. Although biochemical analysis of cyst content was not performed in the present case, we assume that the presence of highly gelatinous and viscous colloid material within loculi in SO may reduce water diffusion.

Many studies showed considerable overlap between the ADC values of cystic components of benign and malignant ovarian lesions[4,5]. Mean ADC values for cystic components of benign ovarian lesions ranged from $1.24\pm0.46\times10^{-3}$ mm²/s to $2.32\pm0.56\times10^{-3}$ mm²/s, and malignant ovarian lesions ranged from $1.64\pm0.48\times10^{-3}$ mm²/s to $2.34\pm0.47\times10^{-3}$ mm²/s[4,5]. There is an overlap in the mean ADC values for the cystic portion of SO compared with the reported ADC values of cystic components of benign and malignant ovarian lesions. On the basis of these results, including the present case, the ADC values for the cystic portion of the SO alone are unlikely to contribute to the differentiation of SO from other cystic ovarian lesions.

When we encounter an ovarian tumor that is composed of both solid and cystic components associated with a dermoid cyst in the same ovary, the differential diagnosis includes a combination of another type of ovarian tumor with a dermoid cyst. Dermoid cysts can occasionally be associated with other types of ovarian tumors of the germinal type, such as SO or carcinoid tumor, or non-germinal tumors such as mucinous tumor, serous tumor, or Brenner tumor[10,19]. Of these, a typical example of an ovarian tumor showing a complex solid and cystic appearance is mucinous cystadenocarcinoma. The solid portion of mucinous cystadenocarcinoma shows high signal intensity on DWI and low signal intensity on the corresponding ADC map image (i.e. a low ADC value)[8]. Furthermore, when we encounter a case of a dermoid cyst with an abundant solid component, malignant transformation of the dermoid cyst should be included in the differential diagnosis. The most common type of

malignant transformation of dermoid cyst is squamous cell carcinoma, but adenocarcinoma, malignant melanoma, sarcoma, and other forms have been reported[10]. Squamous cell carcinoma and other malignant elements appear as a cauliflower-like mass protruding into the cavity of the dermoid cyst as a mural nodule. When more advanced, extra-capsular growth occurs, and these malignant elements invade directly to the adjacent organs[20].

In conclusion, a case of SO was described, and MRI findings, focused on DWI findings, were discussed. The solid portion of the SO showed a high ADC value, indicating unrestricted diffusion, and each loculus of SO showed different ADC values due to the different viscosities of the cyst contents in each loculus. These unique and characteristic DWI findings may serve as a helpful sign in providing the correct diagnosis of SO, when DWI findings are interpreted in conjunction with conventional MRI findings.

References

1. Qayyum A. Diffusion-weighted imaging in the abdomen and pelvis: concepts and applications. Radiographics 2009;29:1797-1810.
2. Fujii S, Kakite S, Nishihara K, Kanasaki Y, Harada T, Kigawa J, et al. Diagnostic accuracy of diffusion-weighted imaging in differentiating benign from malignant ovarian lesions. J Magn Reson Imaging 2008;28:1149-1156.
3. Takeuchi M, Matsuzaki K, Nishitani H. Diffusion-weighted magnetic resonance imaging of ovarian tumors: differentiation of benign and malignant solid components of ovarian masses. J Comput Assist Tomogr 2010;34:173-176.
4. Nakayama T, Yoshimitsu K, Irie H, Aibe H, Tajima T, Nishie A, et al. Diffusion-weighted echo-planar MR imaging and ADC mapping in the differential diagnosis of ovarian cystic masses: usefulness of detecting keratinoid substances in mature cystic teratomas. J Magn Reson Imaging 2005;22:271-278.
5. Katayama M, Masui T, Kobayashi S, Ito T, Sakahara H, Nozaki A, et al. Diffusion-weighted echo planar imaging of ovarian tumors: is it useful to measure apparent diffusion coefficients? J Comput Assist Tomogr 2002;26:250-256.
6. Thomassin-Nagarra I, Darai E, Cuenod CA, Fournier L, Toussaint I, Marsault C, et al. Contribution of diffusion-weighted MR imaging for predicting benignity of complex adnexal masses. Eur Radiol 2009;19:1544-1552.
7. Koc Z, Erbay G, Ulusan S, Seydaoglu G, Aka-Bolat F. Optimization of b value in diffusion-weighted MRI for characterization of benign and malignant gynaecological lesions. J Magn Res Imaging 2012;35:650-659.
8. Li W, Chu C, Cui Y, Zang P, Zhu M. Diffusion-weighted MRI: a useful technique to discriminate benign versus malignant ovarian surface epithelial tumors with solid and cystic components. Abdom Imaging 2012;37:897-903.
9. Zhang H, Zhang GF, He ZY, Li ZY, Zhu M, Zhang GX. Evaluation of primary adnexal masses by 3T MRI: categorization with conventional MR imaging and diffusion-weighted imaging. J Ovarian Res 2012;5:33.
10. Roth LM, Talerman A. Recent advances in the pathology and classification of ovarian germ cell tumors. Int J Gynecol Pathol 2006;25:305-320.
11. Roth LM, Talerman A. The enigma of struma ovarii. Pathology 2007;39:139-146.
12. Savelli L, Testa AC, Timmerman D, Paladini D, Ljungberg O, Valentin L. Imaging of gynecological disease (4): clinical and ultrasound characteristics of struma ovarii. Ultrasound Obstet Gynecol 2008;32:210-219.
13. Shanbhogue AK, Shanbhogue DK, Prasad SR, Surabhi VR, Fasih N, Menias CO. Clinical syndromes associated with ovarian neoplasms: a comprehensive review. Radiographics 2010;30:903-919.
14. Ikeuchi T, Koyama T, Tamai K, Fujimoto K, Mikami Y, Konishi I, et al. CT and MR features of struma ovarii. Abdom Imaging 2012;37:904-910.
15. Joja I, Asakawa T, Mitsumori A, Nakagawa T, Hiraki Y, Kudo T, et al. Struma ovarii: appearance on MR images. Abdom Imaging 1998;23:652-656.
16. Kuzuhara Y, Takeshita T, Shimono T, Koyama K, Honda K, Wakasa K, et al. A case of struma ovarii with predominantly solid component. Japanese Journal of Clinical Radiology 2012;57:978-982 (in Japanese).
17. Okada S, Ohaki Y, Kawamura T, Hayashi T, Kumazaki T. Cystic struma ovarii: imaging findings. J Comput Assist Tomogr 2000;24:413-415.

18. Takeshita T, Ninoi T, Doh M, Hashimoto S, Inoue Y. Diffusion-weighted magnetic resonance imaging in tubo-ovarian abscess: a case report. Osaka City Med J 2009;55:109-114.
19. Okada S, Ohaki Y, Ogura J, Ishihara M, Kawamura T, Kumazaki T. Computed tomography and magnetic resonance imaging findings in cases of dermoid cyst coexisting with surface epithelial tumors in the same ovary. J Comput Assist Tomogr 2004;28:169-173.
20. Kido A, Togashi K, Konishi I, Kataoka ML, Koyama T, Ueda H, et al. Dermoid cysts of the ovary with malignant transformation: MR appearance. AJR Am J Roentgenol 1999;172:445-449.